Available online at www.sciencedirect.com

ScienceDirect

International Journal of Heat and Mass Transfer 51 (2008) 4926–4939

International Journal of HEAT and MASS TRANSFER

www.elsevier.com/locate/ijhmt

Two-phase pressure drops in a helically coiled steam generator

Lorenzo Santini *, Andrea Cioncolini [1], Carlo Lombardi, Marco Ricotti

Nuclear Engineering Department, Politecnico di Milano, Via Ponzio 34/3, 20133 Milano, Italy

Received 26 February 2007
Available online 21 April 2008

Abstract

An experimental investigation regarding two-phase diabatic pressure drops inside a helically coiled heat exchanger have been carried out at SIET thermo-hydraulics labs in Piacenza (Italy). The experimental campaign is part of a wide program of study of the IRIS innovative reactor steam generator. The test section consists of an AISI 316 stainless steel tube, 32 m length, 12.53 mm inner diameter, curved in helical shape with a bend radius of 0.5 m and a helix pitch of 0.8 m, resulting in a total height of the steam generator tube of 8 m. The explored operating conditions for two-phase flow experiences range from 192 to 824 kg/m^2 s for the mass flux, from 0 to 1 for the quality, from 1.1 to 6.3 MPa for the pressure, from 50 to 200 kW/m^2 for the heat fluxes. A frictional two-phase pressure drops correlation, based on an energy balance of the two-phase mixture and including the 940 experimental points, is proposed. Comparison with existing correlations shows the difficulty in predicting two-phase pressure drops in helical coil steam generators.

Keywords: Coils; Helically coiled pipes; Steam generator; Two-phase flow; Pressure drops

1. Introduction

Heat exchangers are one of the most common technological device applied in power, chemical and food processing industries. Many options are available for obtaining compactness and efficiency in exchanging thermal power. In the field of tubular heat exchangers one possible way for reducing the space occupied by the exchanger is by bending tube axis in helicoidal shape. This option is particularly suitable when construction simplicity is needed and when the geometry of the place in which the exchanger has to be housed is the cylindrical one. Many advantages derive from this disposition, such as an excellent behaviour in presence of severe thermal expansions; in fact the helical shape allows the exchanger to behave as a spring, thus accommodating the stresses due to the expansions. Moreover the exchanger has the possibility of working locally in the cross-flow disposition and globally in counter-flow (the so called cross-counter principle applied in many shell and tube exchangers), thus combining all the positive aspects of the two arrangement. Helically coiled heat exchangers in the multi-start disposition has no internal baffle leakage problems and are little sensitive to flow maldistributions [1]. However, some difficulties could rise in the manufacturing process and in the bundle fabrication phase, thus increasing costs.

In the past many industrial applications of helically coiled tube-bundle heat exchangers have been realized: natural gas liquefaction apparatus [1], solar energy concentrator receivers [2] and many steam generators for nuclear power plants (e.g. Otto Hahn nuclear ship, SuperPhoenix fast reactor, AGR , Fort St. Vrain HTGR, THTR-300 etc.). Up to now there are several projects in nuclear industry for electricity production involving helically coiled steam generators [3].

The presence of two new geometrical variables, such as coil diameter and coil pitch, renders single-phase thermohydraulics phenomena in coiled ducts more complex than

* Corresponding author. Tel.: +39 02 2399 6330; fax: +39 02 2399 6309. *E-mail address:* lorenzo.santini@polimi.it (L. Santini).

[1] Present address: Heat and Mass Transfer Laboratory, EPFL-École Polytechnique Fédérale de Lausanne, EPFL-STI-IGM-LTCM, Mail 9, CH-1015 Lausanne, Switzerland.

0017-9310/$ - see front matter © 2008 Elsevier Ltd. All rights reserved.
doi:10.1016/j.ijheatmasstransfer.2008.02.034

Nomenclature

A	inner cross sectional area of the tube (m^2)
D	helix diameter (m)
d	tube inner diameter (m)
f	friction factor (Fanning)
F	parameter in Ruffel's correlation
G	mass flux (kg/m^2s)
g	gravity acceleration (m/s^2)
K	quality multiplier
L	tube length (m)
MEM	mean error
N	number of experimental points
p	pressure (Pa)
R_p	reduced pressure
Re	Reynolds number
RMS	root mean square error
s	curvilinear abscissa (m); tube perimeter (m)
v	specific volume (m^3/kg)
x	thermodynamic equilibrium quality
y	parameter in Ruffel's correlation
z	vertical elevation (m)

Greek symbols

α	volumetric gas fraction (void fraction)
τ	tangential stress (Pa/m^2)
ρ^*	photographic density (kg/m^3)
Δ	difference
ΔP_0	frictional pressure drops with liquid flowing alone with total flow rate
μ	viscosity ($Pa \times s$)
ξ	two-phase multiplier in Chen's correlation
θ	tube inclination (to horizontal direction) (deg)
ρ	density (kg/m^3)
ψ	two-phase multiplier in Guo's correlation
Φ_{lo}^2	two-phase multiplier

Subscripts

a	accelerative
c	coil
calc	calculated value
E	referred to energy balance
exp	experimental value
f	frictional
g	vapour phase; gravitational
l	liquid phase
lo	liquid only
m	mixture (referred to the homog. model)
M	referred to momentum balance
str	straight
tp	two-phase
w	wall

in straight ones. However, as a result of relatively wide experimental campaigns, correlations of pressure drops and heat transfer coefficients of acceptable validity are available mainly in the single-phase regime [4]. Moreover, as happens in straight tubes, two-phase flow behaviour is further complicated, also because besides pressure drops and heat transfer coefficients, the knowledge of dry out power and thermo-hydraulics instabilities is needed. In particular, no general correlation for two-phase pressure drops in coils, valid for a wide range of physical parameters, is available till now, while a certain number is proposed for specific and limited ranges. However, none of them tries to correlate pitch effect, even if it is supposed to be in general moderate.

In the present work single and two-phase pressure drops in diabatic conditions are measured in a helically coiled 32 m long steam generator electrically heated with inner diameter of 12.53 mm, coil diameter of 1 m and 0.8 m of pitch. This tube is representative of the steam generator foreseen for the IRIS reactor [5]. The explored operating conditions for two-phase diabatic pressure drops range from 195 to 824 $kg/m^2\,s$ for the mass flux, from 0 to 1 for the quality, from 1.1 to 6.3 MPa for the pressure, from 50 to 200 kW/m^2 for the heat flux. Two-phase pressure drops data reduction allowed to extend the range of explored conditions offered in free literature and a simple correlation for their prediction is proposed in the paper.

The synthesis of the data coming from the experimental campaign gave also a correlation for calculating single-phase Fanning friction factor in the tested tube up to Reynolds number of 6.34×10^5. This result allow to fill the shortage of informations in literature regarding high Reynolds numbers single-phase frictional pressure drops in coiled tubes.

2. Review of pressure drops correlations in helical tubes for two-phase flow

In the last few years Chinese researchers has given an important contribution to the knowledge of two-phase pressure drops in helically coiled heat exchangers. In a recent article Guo et al. [6] have compared the available correlations, showing the difficulties of predicting two-phase pressure drops by different formulas. The authors have tested two electrically heated coiled steam generators with several tube axis inclinations, putting in light the strong effect of this parameter on two-phase pressure drops. The investigated conditions were: steam–water mixture, tube of 10 mm of inner diameter, D/d of 13 and 25; pressure 0.5–3.5 MPa, mass flux 150–1760 $kg/m^2\,s$, quality 0–1.2. They obtained the following correlation:

$$\Delta P = \Phi_{lo}^2 \Delta P_0 \tag{1}$$

With

$$\Phi_{lo}^2 = 142.2\psi\left(\frac{P}{P_{cr}}\right)^{0.62}\left(\frac{d}{D}\right)^{1.04}\left[1 + x\left(\frac{\rho_l}{\rho_g} - 1\right)\right] \tag{2}$$

$$\psi = 1 + \frac{x(1-x)(1000/G - 1)(\rho_l/\rho_g)}{1 + x(\rho_l/\rho_g - 1)} \quad \rightarrow \ G \leqslant \ 1000\ \text{kg/m}^2\ \text{s} \tag{3}$$

$$\psi = 1 + \frac{x(1-x)(1000/G - 1)(\rho_l/\rho_g)}{1 + (1-x)(\rho_l/\rho_g - 1)} \quad \rightarrow \ G \geqslant \ 1000\ \text{kg/m}^2\ \text{s} \tag{4}$$

Ruffell [7] tested three coils curvatures with electrically heated test sections for AGR (advanced gas reactors) performances prediction. The explored thermo-hydraulics conditions were the following: pressures from 6.0 to 18 MPa, mass fluxes from 300 to 1800 kg/m^2 s, tube diameters from 10.7 to 18.6 mm and D/d between 6.25 and 185. The proposed correlation for the liquid only frictional multiplier is the following:

$$\Phi_{lo}^2 = (1 + F)\frac{v_m}{v_l} \tag{5}$$

In which

$$\begin{aligned} F = \sin\left(\frac{1.16G}{10^3}\right)&\left\{0.875 - 0.314y - \frac{0.74G}{10^3}(0.152 - 0.07y)\right. \\ &\left. - x\left(\frac{0.155G}{10^3} + 0.7 - 0.19y\right)\right\} \\ &\times \{1 - 12(x - 0.3)(x - 0.4)(x - 0.5)(x - 0.6)\} \end{aligned} \tag{6}$$

and

$$y = \frac{D}{100d} \tag{7}$$

The author suggests the application of a specific correlation for void fraction computation in order to calculate accelerative and gravitational pressure drops in conjunction with Eq. (5).

Unal and co-workers [8] tested three coiled tubes with sodium heating in order to investigate dry out occurrence and pressure drops for a LMFBR (Liquid Metal Fast Breeder Reactor) steam generator. The investigated conditions were: steam–water mixture, tube of 18 mm of inner diameter, D/d of 39 and 83, pressures 14.9–20.1 MPa, mass flux 296–1829 kg/m^2 s, quality 0.15–1.0. They obtained the following correlation:

$$\Delta P = 2(1 + b_1 b_2) f_l L G^2/(d\rho_l) \tag{8}$$

in which

$$b_1 = 3850x^{0.2}R_p^{-1.515}Re_l^{-0.758} \tag{9}$$

$$b_2 = 1 + Re_l^{0.1}(3.67 - 3.04R_p) \times [\exp(-0.014D/d) - \exp(-2D/d)] \tag{10}$$

f_l is the friction factor of the liquid phase if flowing alone with the same total flow rate and R_P is the reduced pressure (P/P_{cr}). The test section was fluid heated.

Chen et al. [9] tested three-coiled tubes with an air–water mixture flow. The investigated conditions were: tube of 18 mm of inner diameter, D/d of 13.1, 24.8 and 50.4, pressure 4.2–22 MPa, mass flux 400–2000 kg/m^2 s. They obtained the following correlation:

$$\Delta P = \xi \Delta P_0 \tag{11}$$

in which ΔP_0 is the frictional pressure drop when all the flow rate is supposed liquid and the two-phase multiplier is defined as follows:

$$\begin{aligned} \xi = 2.06\left(\frac{d}{D}\right)^{0.05} Re_{tp}^{-0.025}&\left[1 + \alpha\left(\frac{\rho_g}{\rho_l} - 1\right)\right]^{0.8} \\ \times &\left[1 + x\left(\frac{\rho_l}{\rho_g} - 1\right)\right]^{1.8}\left[1 + \alpha\left(\frac{\mu_g}{\mu_l} - 1\right)\right]^{0.2} \end{aligned} \tag{12}$$

The inconvenience of this formula is the need of knowing the volumetric gas fraction, α.

Zhao et al. [10] tested one coiled electrically heated tube with horizontal axis obtaining results both on convective coefficients and two-phase frictional pressure drops. The investigated conditions were: steam–water mixture, tube of 9 mm of inner diameter, D/d of 32.5; pressure 0.5–3.5 MPa, quality 0–0.95, mass flux 236–943 kg/m^2 s. They obtained the following correlation:

$$\Delta P = \Phi_{lo}^2 \Delta P_0 \tag{13}$$

with

$$\Phi_{lo}^2 = 1 + \left(\frac{\rho_l}{\rho_g} - 1\right)\left[0.303x^{1.63}(1-x)^{0.885}Re_{lo}^{0.282} + x^2\right] \tag{14}$$

The authors have tested one coil only, so that the correlation does not contain any dependence on coil curvature. Re_{lo} refers to the Reynolds number calculated with the whole flow rate supposed to be liquid.

3. Facility and test section description

The test section is framed into an open loop facility built inside the boiler building of the "Emilia" power station in Piacenza where SIET labs [11] are located. The facility is made by a supply section (Fig. 1) and a test section (Fig. 2).

The supply section feeds demineralized water from a tank to the test section, by means of a centrifugal booster pump and a feed-water pump, i.e., a volumetric three-cylindrical pump with a maximum head of about 200 bar driven by an asynchronous three-phases motor. After the reciprocating pump a bypass line with a control valve allows the

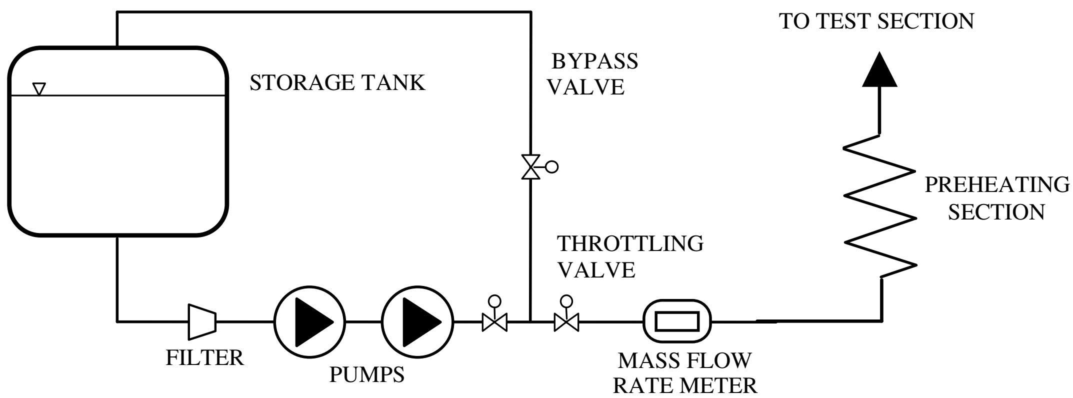

Fig. 1. Scheme of the supply section.

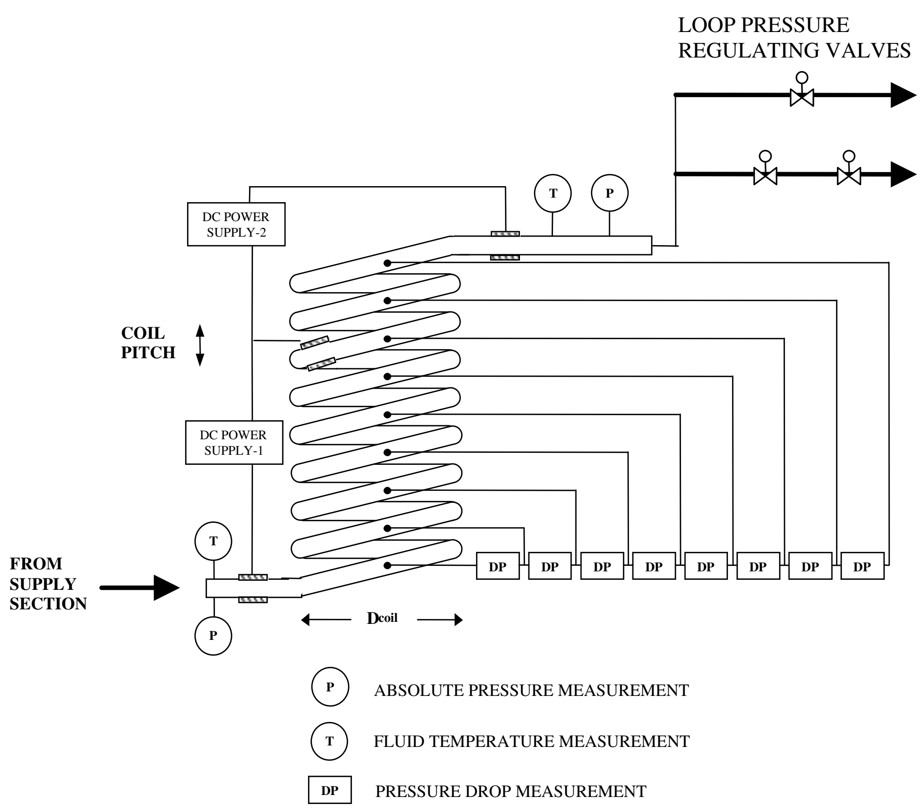

Fig. 2. Scheme of the test section.

operator to impose to the circuit the desired flow rate. The bypass line is followed by a throttling valve whose scope is to introduce a strong localized pressure drop in order to avoid any eventual dynamic instability (density wave type) of the test section when it is powered.

Booster pump sucks water from a large capacity tank charged with demineralised water, with a measured mean electrical conductivity of 1.5 μS/cm, obtained with a ionic exchanger resin bed.

An electrically heated coiled tube pre-heater is located beyond the flow meter, but before the test section, and allows to create the desired temperature at test section inlet.

The test section in Fig. 2 is electrically heated via Joule effect by DC current. Two distinct, independently controllable and contiguous sections are provided: the first one, with a length of 24 m, simulates the subcooling zone and the two-phase zone of the steam generator, while the second, of 8 m length, simulates the superheating zone.

At the end of the plant three valves, two with automatic air operated pressure control and one manually operated, have the scope of controlling the proper pressure of the facility by throttling the mixture before it is discharged to the atmosphere.

The test section consists of a stainless steel tube, curved in helical shape and connected to a lower and a upper header. The main data of the steam generator tube are listed in Table 1.

Measures made with digital calibre with an accuracy of 1/100 mm on tube inner diameter on a sample straight tube of the same verges used for the test section, showed a maximum difference between measured values and nominal one of 0.44%, underlining the validity of nominal value.

Further measures taken along the coiled test section, namely at the beginning, in the middle and at the end, on tube outer diameters showed an ovalization (here defined as the ratio between the difference of two orthogonal diameters and tube outer diameter nominal value) of tube outer diameter that never exceed 1.22%. This ovalization was considered negligible in hydraulic and electric calculations, i.e., the nominal straight values of tube inner and outer diameters were considered valid for all the calculations regarding the test section.

Tube inner surface roughness have been measured on the same straight sample used for inner and outer diameters measures. A total of six measures, three on one side and three on the other of the sample, gave a mean roughness of 3.08 μm (maximum value 3.5 μm, minimum value 2.5 μm).

An accurate measurement of the flow rate is obtained by a Coriolis flow-meter, having a maximum error of about 1%, in the range of the explored flow rates.

Bulk temperatures are measured with type "K" thermocouple with insulated junction. The thermocouples have 1.5 mm diameter and are directly immersed into the fluid, the maximum absolute uncertainty in the range of the explored temperatures is 0.7 °C. All the measurement devices have been tested and calibrated at the certified SIET labs (SIT certified).

The water pressure at heating section inlet is measured by an absolute pressure transducer with a 100 bar range, and a maximum error of about 0.1%.

Table 1
Test section main data

Tube material	SS AISI 316
Inner diameter, d (mm)	12.53
Outer diameter (mm)	17.24
Coil diameter, D (mm)	1000
Coil pitch (mm)	800
Tube length (m)	32
Steam generator height (m)	8
Number of pressure taps	9

Nine pressure taps are disposed nearly every four meters along the coiled tube and eight differential pressure transducers (maximum error of about 0,4%) connect the pressure taps. The detailed distances between the taps are reported in the next table (Table 2). All the measurements are acquired by a multi-channel data acquisition system with a frequency of acquisition of 4 Hz and stored into a computer.

The steam generator tube is carefully insulated with rock wool, and the small thermal losses were previously determined with dedicated experiences. This losses were measured by evaluating the flow rate and the temperature drop of hot pressurized water flowing into the steam generator and their value were correlated with the tube metal temperature.

Electric power is supplied to the steam generator via Joule effect using low voltage (a hundred Volts)-high amperage current. The electric power generator is the coupling of a AC transformer, with a Chopper that convert alternate current into direct current.

Electrical power was calculated via separate measurement of current (by a shunt) and voltage drop along the test section by a voltmeter. The uncertainty in steam generator power balances was estimated to be 2.5%.

4. Facility operation and data reduction

During two-phase flow experiences, once the desired flow rate imposed to the plant, power were given to the pre-heater in order to obtain the proper test section inlet subcooling. The first 24 m of the test section were powered in order to completely evaporate the mixture. A proper actuation of end-plant throttling valves allowed to obtain the desired open loop pressure.

The results obtained are useful also for dry out inception evaluation, but will not be presented in this paper.

The thermodynamic equilibrium quality of the mixture flowing along the tube is calculated via an energy balance between the electrical power generated in the tube wall and the estimated thermal losses towards the environment.

The local reference quality between two pressure taps is the arithmetic mean of the qualities calculated in correspondence of the two taps. The local reference pressure between the two taps is the arithmetic mean of the pressures measured in correspondence of the two taps. Liquid and vapour saturation enthalpies are calculated at the local pressure between the taps using NIST standard reference database.

For superheated steam diabatic pressure drops investigation, electrical power were given at the last 8 m of the test section. Steam properties, as for mixture properties, have

Table 2
Pressure taps distribution along the test section

	Tap 1	Tap 2	Tap 3	Tap 4	Tap 5	Tap 6	Tap 7	Tap 8	Tap 9
Distance from test section inlet (mm)	200	5173	9186	13,148	17,141	21,643	25,586	29,088	32,059

been evaluated at the average values of pressure and temperatures between two pressure taps.

Mass flux is obtained as the ratio between flow rate measurement and tube inner cross-sectional area based on tube nominal inner diameter.

5. Pressure drops investigation

In general, four fundamental reasons require to obtain a reasonable accuracy in predicting the pressure drops in a steam generator:

– calculation of the total head to be supplied by the feedwater pump of the Rankine cycle: the pressure drops in the steam generator of a power plant may represent a significant portion of the total head (e.g., a supercritical fossil fuel power station with a pressure of 250 bar at turbine inlet could have more than 60 bar of pressure drops in the steam generator);
– calculation of the thermodynamic conditions of the steam at turbine inlet: turbine efficiency optimisation is based on design values of inlet pressure and temperature, on which velocity triangles depend, so that their accurate prediction is of paramount importance;
– dimensioning the inlet orifice for damping the two-phase flow oscillations, hence avoiding flow pressure instabilities;
– calculation of pinch point temperature drop: the temperature drop between primary fluid and secondary one where the two streams reach the minimum temperature difference (pinch point) is of paramount importance for steam generator sizing. Secondary side pinch point local temperature can be predicted only if an accurate evaluation of local saturation pressure is known and this can be done with a proper steam generator pressure drops modelling.

Table 3
Thermal-hydraulic conditions for single-phase pressure drop measurements

Reynolds number	Pressure, P (bar)	Thermal flux (kW/m^2)	Fluid
1.3e + 4–6.34e + 5	5–60	50–200	Water–steam

In the experimental campaign both single-phase and two-phase pressure drops in diabatic conditions have been investigated within a range of possible operating conditions for the steam generator.

5.1. Single-phase diabatic pressure drops

The thermal-hydraulics conditions adopted for the single-phase pressure drop experimental campaign are summarized in Table 3.

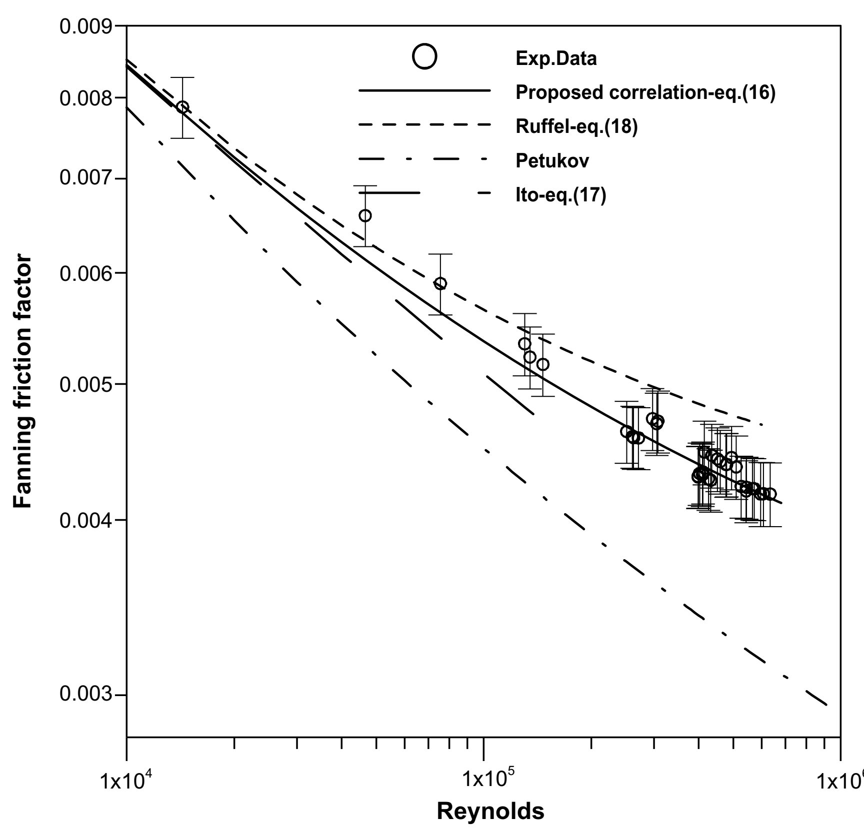

Fig. 3. Fanning friction factor as a function of Reynolds number.

In differential terms, the total losses (dP) can be subdivided into the frictional term (dP_f), the acceleration term (dP_a) and the gravitation term (dP_g). For a single-phase fluid it reads

$$dP = dP_f + dP_g + dP_a = 2f\frac{G^2}{\rho d}ds + \rho g dz + G^2 dv \tag{15}$$

Table 4
Thermal-hydraulic experimental conditions for two-phase flow pressure drops

Mass flux, G (kg/m^2 s)	Pressure, P (bar)	Thermal flux (kW/m^2)	Quality	D/d
192–811	11–63	50–200	$0 < x < 1$	79.8

where f is the Fanning friction factor, dv is the variation of specific volume along that tube and dz is the vertical elevation corresponding to the ds increase of the curvilinear abscissa along the tube (for vertical straight tubes $dz = ds$). By subtracting the gravitation and the acceleration terms from the measured pressure losses, the friction term is obtained.

Fig. 3 reports the friction factor f as a function of the Reynolds number. The experimental points at low Reynolds numbers were obtained by subcooled liquid flow rates, while at higher Re numbers by superheated steam. In subcooled water the friction factor was obtained by the overall pressure drop for the whole tube for three different conditions (already adopted for thermal losses calibrations). The physical data of water were calculated by

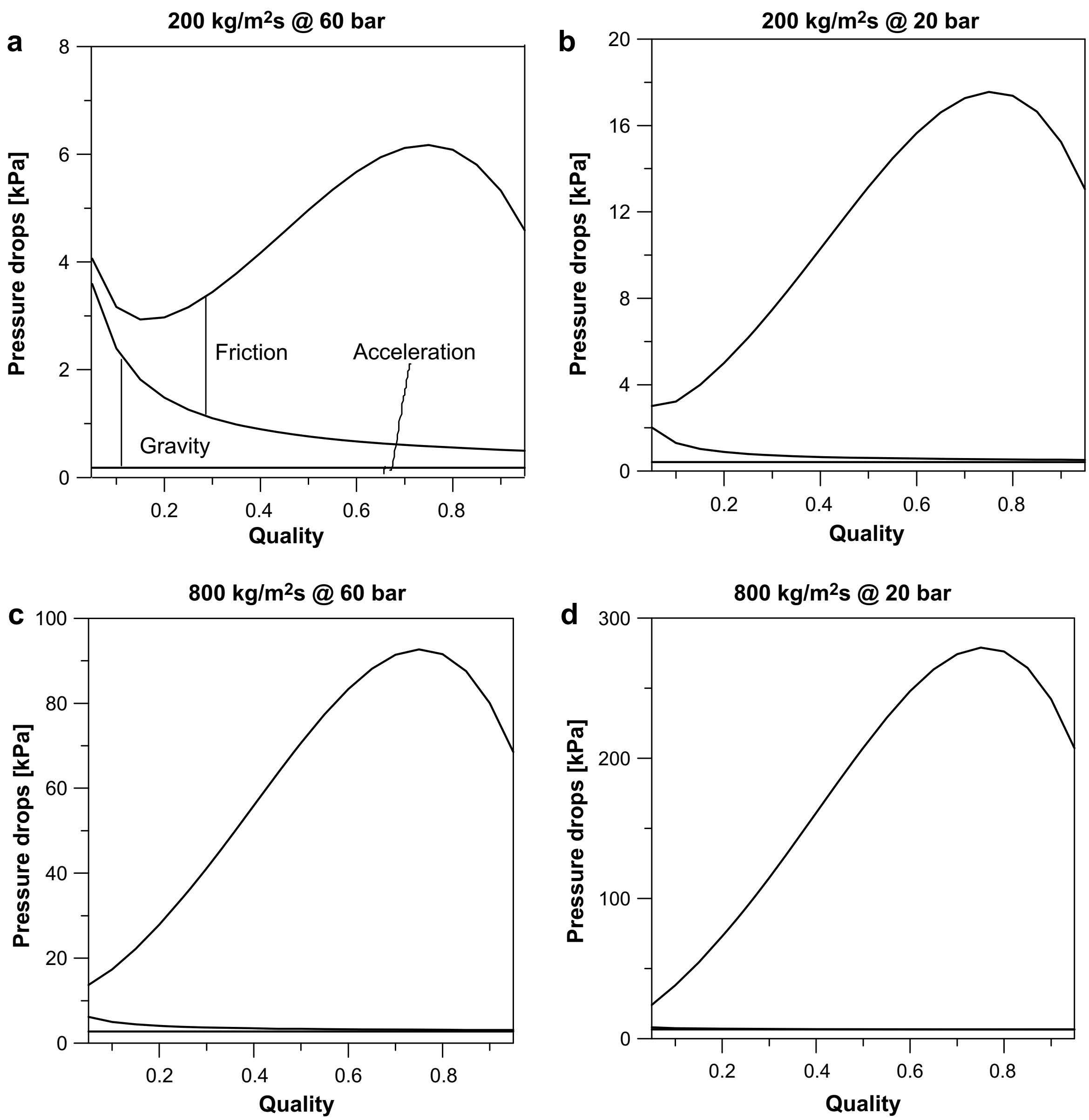

Fig. 4. Comparison between the contribution of gravity, acceleration and friction between two pressure taps for different operative conditions in our exp. facility.

averaging the values of inlet and outlet temperatures which differed of few degrees. The superheated steam data are those measured in the last portion of the test section (taps 8 and 9), and the physical data were assumed in the same manner adopted for subcooled water; however in this case the temperature difference was higher and approximately 30 °C. Due to the relatively small impact of the accelerative term in the data obtained with vapour (less then 25%), the results are applicable as adiabatic data. The 36 experimental data are correlated by the following empirical equation:

$$f = 0.00206 + 0.085Re^{-0.278} \tag{16}$$

with a root mean square (RMS) error of 2.0%, within $13{,}000 < Re < 634{,}000$.

The experimental data lie within two existing known correlations for coil tube geometries, namely the Ito's correlation [12] valid for Re numbers up to a maximum of 150,000

$$f_{\mathrm{Ito}} = 0.076\ Re^{-0.25} + 0.00725\left(\frac{D}{d}\right)^{-0.5} \tag{17}$$

and the Ruffel [7] correlation obtained by AGR (advanced gas reactors) tests and valid for a maximum Reynolds number of 600,000:

$$f_{\mathrm{Ruffel}} = 0.0375 + 0.633\left(\frac{D}{d}\right)^{-0.275} Re^{-0.4} \tag{18}$$

In order to compare these data with straight tube friction pressure losses, the Petukov correlation [13] is plotted as well. By comparing our data with these correlations it is interesting to observe that these are in between. The comparison with Ito correlation is limited to Reynolds numbers lower than 150,000, which is the maximum value of Ito's validity range. Finally it can be observed that for the higher Reynolds number tests, the tube roughness may play a significant role, and this can be a possible explanation for the different behaviour that our data manifest with respect to Ruffel correlation.

5.2. Two-phase diabatic pressure drops

The thermal-hydraulic conditions for the two-phase flow pressure drops investigation are reported in Table 4.

In two-phase flow with the hypothesis that both phases have a flat velocity distribution, pressure drops can be expressed both by a momentum balance [14]:

$$\mathrm{d}P_{\mathrm{M}} = G^2\mathrm{d}\left[\frac{x^2}{\alpha\rho_{\mathrm{g}}} + \frac{(1-x)^2}{(1-\alpha)\rho_{\mathrm{l}}}\right] + \tau_{\mathrm{w}}\frac{s}{A}\mathrm{d}s + \rho^* g \cdot \mathrm{d}z \tag{19}$$

and by an energy balance

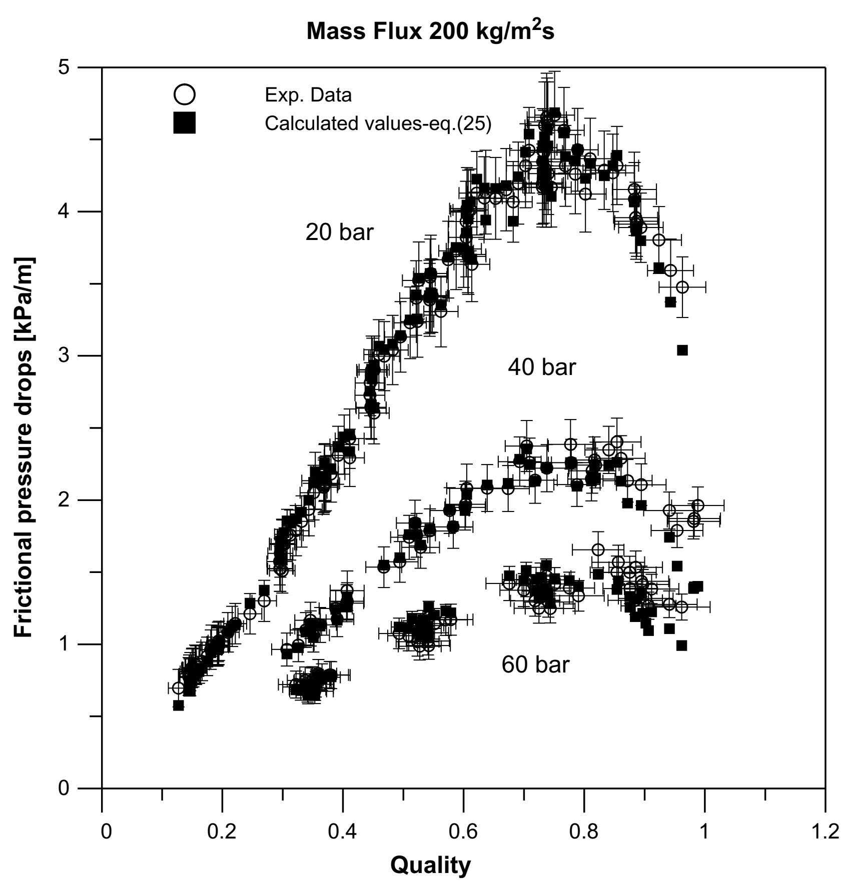

Fig. 5. Two-phase flow frictional pressure drops, at fixed mass flux (200 kg/m^2 s).

$$dP_E = \frac{1}{2}\rho_m G^2 d\left[\frac{x^3}{\alpha^2\rho_g^2} + \frac{(1-x)^3}{(1-\alpha)^2\rho_l^2}\right] + \rho_m dR_m + \rho_m g \cdot dz \tag{20}$$

where R_m is the energy dissipated per unit mass in the fluid flow due to irreversibility, x is the equilibrium thermodynamic quality, α is the volumetric gas fraction, ρ^* is the real density (photographic density) given by:

$$\rho^* = \alpha\rho_g + (1-\alpha)\rho_l \tag{21}$$

and ρ_m is the flow rate mixture density (identical to the homogeneous value):

$$\rho_m = \frac{1}{v_m} = \left(\frac{x}{\rho_g} + \frac{1-x}{\rho_l}\right)^{-1} \tag{22}$$

Eqs. (19) and (20) are obtained with a one dimensional separated phases model in which each phase is imagined occupying a definite portion of tube cross-sectional area. Furthermore the flow is assumed steady and characteristic mean values of phases densities and velocities are assumed.

The total pressure losses obtained by applying relations (19) and (20) are obviously the same ($dP_M = dP_E$), but different are the relative weight and the physical meanings of the three terms involved.

Again some useful hints referred to the pressure loss terms have to be recalled:

– acceleration term: in the momentum balance, it represents the pressure gradient due to the accelerative recoil of the mixture, while in the energy balance it is the work necessary for varying the kinetic energy of the mixture. The volumetric gas fraction has to be known both in the momentum and in the energy balance equations;
– friction term: in the momentum balance, it represents the tangential stress that the tube wall exerts on the mixture, while in the energy balance it represents the work of the dissipative forces acting inside the mixture inside the channel (conversion of mechanical energy into internal energy due to viscous effect). No explicit information on volumetric gas fraction is necessary for this term;
– gravitation term: in the momentum balance, it is proportional to the photographic density that expresses the weight of the mixture column, while in the energy balance it is proportional to the flow rate mixture density (generally smaller then the photographic one), which has to be taken into account for calculating the work to elevate the mixture column. The volumetric gas fraction has to be known in order to calculate the gravitational term in the momentum balance equation, while this is not required in the energy balance equation, because the flow rate density is identical to the homogeneous density of the mixture, which can be easily calculated.

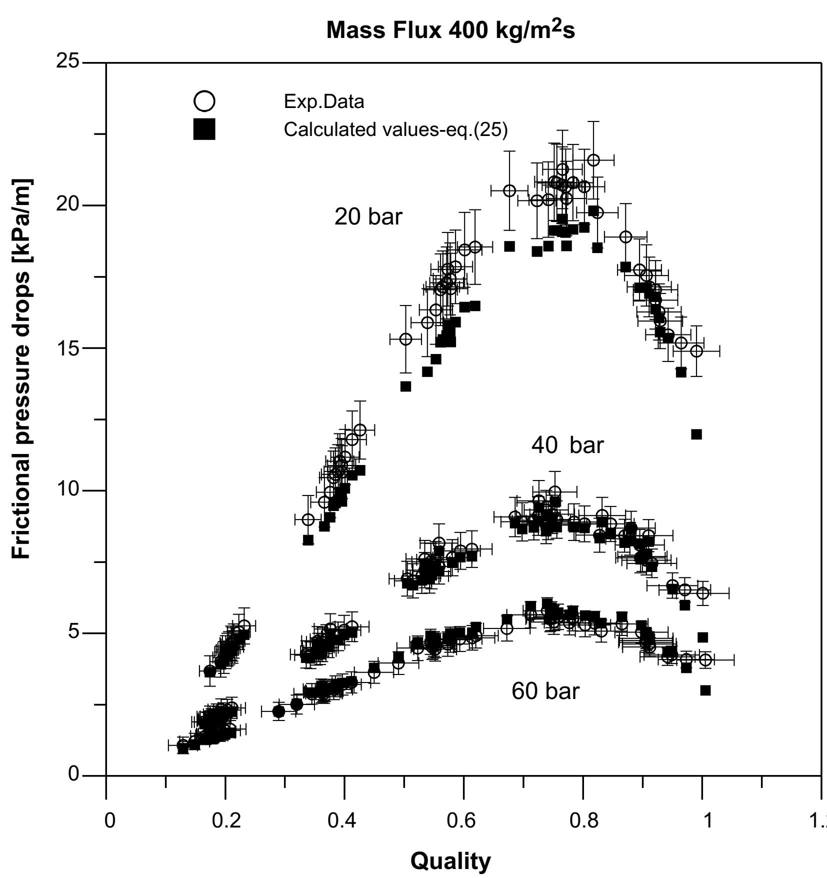

Fig. 6. Two-phase flow frictional pressure drops, at fixed mass flux (400 kg/m^2 s).

Almost all the correlations on two-phase pressure drops in literature adopt the momentum balance approach, an exception is represented by the correlations due to CISE [15] and Lombardi et al. [16] for two-phase pressure drops in vertical upflowing straight tubes. Some advantages derive from the application of the energy balance approach such as the absence of the necessity of introducing volumetric gas fraction for the calculation of the gravitation term and the intrinsically non-negative nature of the frictional term.

Momentum and energy balance approaches coincide in all the three terms of the total pressure drops (friction, gravity and acceleration), if the further hypotheses of no slip between phases and flat velocity profile along the tube radius are introduced, as we will do here, because the lack of knowledge in literature about volumetric gas fraction inside helically coiled tubes.

Once the experimental data have been obtained, the gravitation and the acceleration terms are calculated and subtracted to the measured total pressure losses, hence the remaining friction term is correlated by the system parameters, such as flow rate, quality and pressure.

Therefore, the friction term is obtained from the experimental data by the following equation:

$$\mathrm{d}P_f = \mathrm{d}P_{\text{measured}} - G^2\mathrm{d}v_m - \rho_m \cdot g \cdot \mathrm{d}z \tag{23}$$

The experimental data refer to the average values between two adjacent pressure taps, the distance of which is about 4 m, corresponding to a quality variation of about 16% for our experiences. A typical plot of the three pressure drops terms between two taps is shown in the next figure (Fig. 4a–d) in which the maximum and minimum values of pressures and mass fluxes are represented. As it is possible to observe gravity and acceleration terms, as here supposed, never play a significant role in the overall pressure drops except in the region of the lower qualities for the case with the minimum mass flux and the maximum pressure (Fig. 4a). It is thus confirmed the major importance of the frictional term in nearly all the explored range of operative conditions for our test section, thus underlining the small importance that volumetric gas fraction knowledge plays in our data reduction.

The empirical relationship correlating the friction term by the independent variables has the following functional structure:

$$\mathrm{d}P_f = \mathrm{d}P_{\mathrm{f}}(P, x, G) \tag{24}$$

The following correlation was chosen:

$$\mathrm{d}P_{\mathrm{f}} = K(x)\frac{G^{1.91}v_{\mathrm{m}}}{d^{1.2}}\mathrm{d}z \tag{25}$$

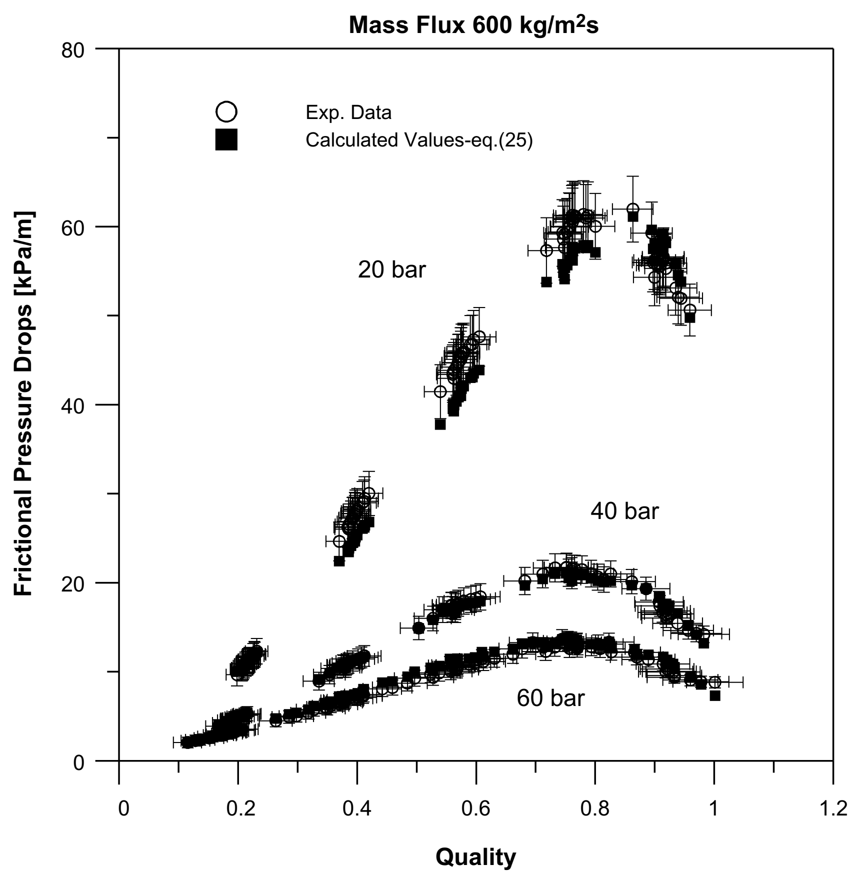

Fig. 7. Two-phase flow frictional pressure drops, at fixed mass flux (600 kg/m^2 s).

where $K(x)$ is a multiplier that takes into account the effect of quality. Since only one tube inner diameter has been investigated, its effect has been assumed identical to that for straight tubes as in Lombardi's et al. work [16]. By minimising the errors we obtained:

$$K(x) = -0.0373x^3 + 0.0387x^2 - 0.00479x + 0.0108 \tag{26}$$

The mass flux effect on two-phase friction pressure drops ($\Delta P_f^{\mathrm{TwoPhase\_coils}} \propto G^{1.91}$), is higher than that in straight smooth tubes both in single-phase ($\Delta P_f^{\mathrm{SinglePhase\_straight}} \propto G^{1.8}$) and two-phase ($\Delta P_f^{\mathrm{TwoPhase\_straight}} \propto G^{1.5}$). This seems to confirm the increased dissipation effect of tube bending, which induces both secondary flows and stratifications in the mixture. Nevertheless it was not possible during this work to parametrically put in light the effect of coil curvature because of only one coil curvature was tested in this experimental campaign.

The experimental results compared with the calculations due to Eq. (25) are plotted in Figs. 5–8.

The following comments on the influence of the parameters on pressure drops can be done:

– pressure: an increase in the operating pressure will always decrease the pressure drops, independent from the flow rate and the quality. This is obvious because the pressure increase reduces the specific volume and thus, ceteris paribus, the velocity of the mixture;
– quality: there is a maximum for the frictional pressure losses, increasing up to a corresponding quality value of about 0.8, then decreasing while quality approaches the unity. This apparently unusual behavior was already observed by other authors in straight tubes [17–19] and is probably due to an annular flow situation in which the liquid film progressively becomes too thin to maintain interface waves;
– flow rate: the dissipations increase with flow rate.

Table 5 and Fig. 9 show the number of data collected via the experimental campaign, the experimental conditions and the errors of the correlation (25) with respect to the data.

Mean error (MEM) and the root mean square error (RMS) indicated in Table 4 are defined in the following manner:

$$\mathrm{MEM} = \frac{1}{N} \cdot \sum_{i=1}^{N} \left[\frac{(\Delta P_{\mathrm{calc}} - \Delta P_{\mathrm{exp}})}{(\Delta P_{\mathrm{calc}} \cdot \Delta P_{\mathrm{exp}})^{1/2}} \right]_i \tag{27}$$

$$\mathrm{RMS} = \left(\sum_{i=1}^{N} \frac{\mathrm{MEM}_i^2}{N} \right)^{1/2} \tag{28}$$

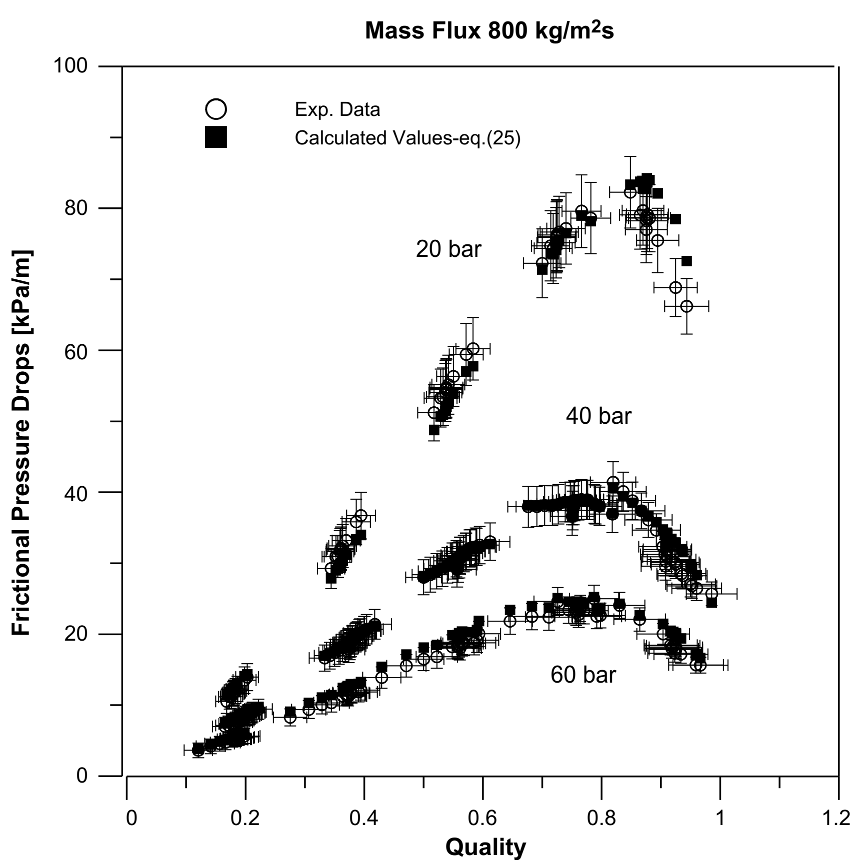

Fig. 8. Two-phase flow frictional pressure drops, at fixed mass flux (800 kg/m^2 s).

Table 5
Two-phase friction pressure drops statistics of proposed correlation

Number of exper'l data	MEM (%)	RMS (%)	Points within ±15%
940	0.11	8.99	94.9%

Table 6
Selected conditions for comparison with other correlations

D/d	G (kg/m^2 s)	x	P (bar)	Number of exper'l data
79.8	800	0.15–0.95	20	55

6. Comparison between two-phase flow pressure drops correlations

The experimental conditions investigated in the present work are quite different from those listed in the previous works found in the literature, thus suggesting to avoid a straightforward application of those correlations to the database obtained by this experimental campaign.

In order to compare different correlations with our experimental results, those proposed by Guo et al. [6], Chen et al. [9], Zhao et al. [10], Unal et al. [8] and Ruffel [7] have been selected and applied to calculate two-phase friction pressure losses for the test section in the range of operative conditions reported in Table 6. We have chosen the maximum mass flux of our investigation in order to reduce the dependence on the volumetric gas fraction correlation applied by others authors in data reduction. The only correlations able to predict the existence of the maximum value of the pressure drops are Zhao's one [10] and Eq. (25). The worst predictions are due to Guo's et al. correlation [6] and the better predictions are due to Eq. (25) and Ruffel's correlation [7]. Two-phase frictional pressure drops predictions are compared in Fig. 10 and Table 7 as a function of mixture quality.

The plot shows significant differences in the predictions, up to a factor of six, thus confirming the difficulty in predicting two-phase pressure drops in helical coil tubes out of the range of experimentally explored conditions.

7. Conclusions

Single-phase and two-phase pressure drops in helical coil steam generator single tube were investigated, by means of a full scale, electrically heated experimental facility. Correlations for both single- and two-phase friction pressure losses were obtained. Data reduction for two-phase frictional pressure drops was obtained by applying the hypotheses of flat velocity profiles and no slip between phases; a correlation that include the 940 experimental data with a RMS of 8.9% and with 94.9% of exp. data within ±15% has been proposed. Two-phase friction pressure drops in our test section showed to be proportional on

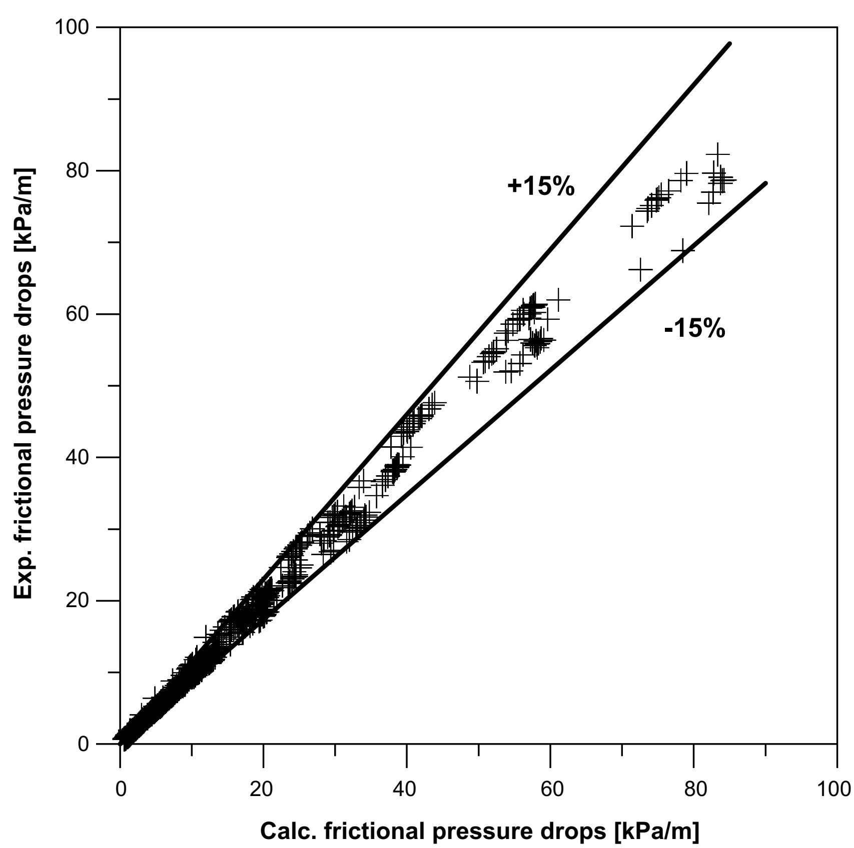

Fig. 9. Comparison between the experimental data and the proposed correlation.

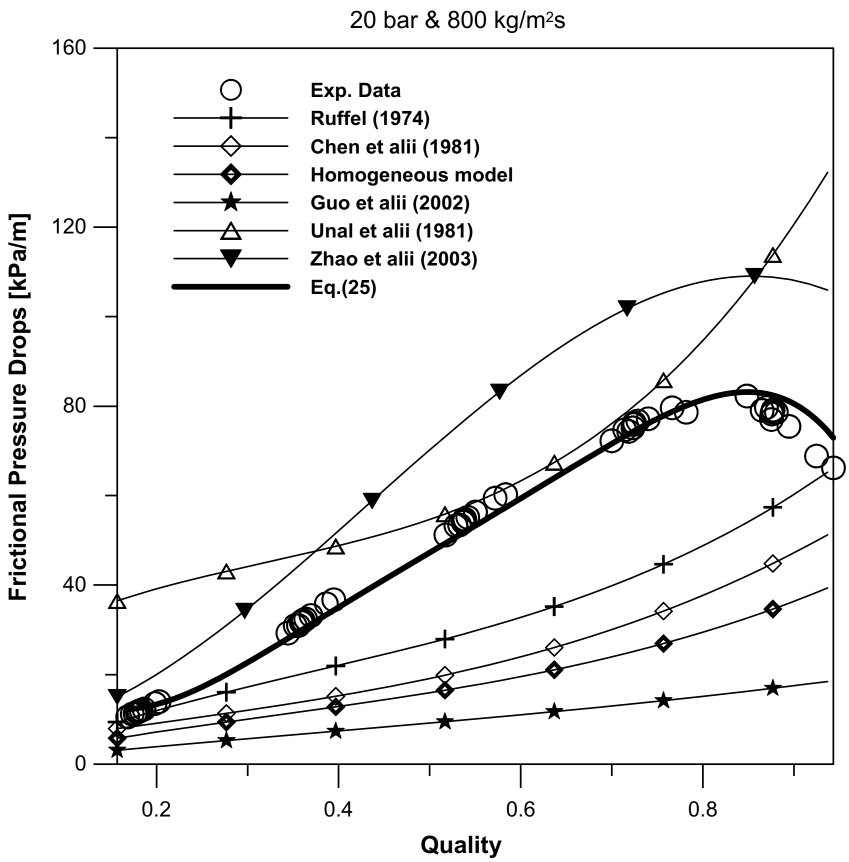

Fig. 10. Comparison among different correlations used for predicting two-phase frictional pressure drops in coiled tubes.

Table 7
Results of comparison with other correlations on two-phase pressure drops in coils

	Eq. (25)	Homog. model	Chen [9]	Zhao [10]	Guo [6]	Unal [8]	Ruffel [7]
MEM	−0.18	−82	−58.1	48.2	−153.7	56.8	−27.9
RMS	6.2	85.7	64.2	48.5	155.9	73.4	36.1

the 1.91 power of flow rate, thus confirming the strong dissipation effect of tube bending.

The comparison with some correlations for two-phase pressure drops in helical coil tubes shows the difficulty in predicting such an important thermal-hydraulic parameter, due to the complexity of the two-phase flow regime induced by the centrifugal forces.

Acknowledgement

The authors are grateful to Gustavo Cattadori, Andrea Achilli and Stefano Gandolfi from SIET labs for their valuable collaboration and deep expertise. The authors are grateful also to Mario Carelli and the colleagues of the IRIS project for the opportunity to work in such a stimulating and challenging adventure. This research activity has been performed in the frame of the FIRB-2001 and COFIN-2004 programmes and with the financial support from the MIUR-Italian Ministry of the University and Research.

References

[1] E.M. Smith, Thermal Design of Heat Exchangers, John Wiley & Sons, 1997.
[2] M.K. Jensen, A.E. Bergles, Critical heat flux in helical coils with a circumferential heat flux tilt toward the outside surface, Int. J. Heat Mass Transfer 25 (1982) 1383–1395.
[3] IAEA, Innovative small and medium sized reactors: design features, safety approaches and R&D trends, Final report of a technical meeting held in Vienna, 7–11 June 2004, May 2005.
[4] V. Gnielinski, Helically coiled tubes of circular cross-section, in: G.F. Hewitt (Ed.), HEDH Design Handbook, Hemisphere Publishing Corporation, 1987.
[5] M.D. Carelli, L.E. Conway, C.L. Kling, L. Oriani, B. Petrović, C.V. Lombardi, M.E. Ricotti, A.C.O. Barroso, J.M. Collado, L. Cinotti, N.E. Todreas, D. Grgić, R.D. Boroughs, H. Ninokata, F. Oriolo, Design and safety of IRIS, an integral water cooled SMR for near term deployment. In innovative small and medium sized reactors: design features, safety approaches and R&D trends. Final report of a technical meeting held in Vienna, 7–11 June 2004, Vienna, IAEA-TECDOC-1451, 2005, pp. 51–74, ISBN 92-0-103205-6.

[6] L.J. Guo, Z. Feng, X. Chen, An experimental investigation of the frictional pressure drop of steam-water two-phase flow in helical coils, Int. J. Heat Mass Transfer 44 (2001) 2601–2610.
[7] A.E. Ruffell, The application of heat transfer and pressure drop data to the design of helical coil once-through boilers, Symp. Multi-Phase Flow Systems, University of Strathclyde, Inst. Chem. Eng. Symp. Ser. 38 (1974) Paper 15.
[8] H.C. Unal, M.L. van Gasselt, P.M. van't Veerlat, Dryout and two-phase pressure drop in sodium heated helically coiled steam generator tubes at elevated pressures, Int. J. Heat Mass Transfer 24 (1981) 285–298.
[9] X.J. Chen, F.D. Zhou, An investigation of flow pattern and frictional pressure drop characteristics of air–water two-phase flow in helical coils, in: Proceedings of the fourth Miami International Conference on Alternate Energy Sources, 1981, pp. 120–129.
[10] L. Zhao, L. Guo, B. Bai, Y. Hou, X. Zhang, Convective boiling heat transfer and two-phase flow characteristics inside a small horizontal helically coiled tubing once-through steam generator, Int. J. Heat Mass Transfer 46 (2003) 4779–4788.
[11] <http://www.siet.it>.
[12] H. Ito, Friction factors for turbulent flow in curved pipes, J. Basic Eng. (1959) 123–134.
[13] F.P. Incropera, D.P. DeWitt, Fundamentals of Heat and Mass Transfer, 4th ed., Wiley, New York, 1996.
[14] J.G. Collier, J.R. Thome, Convective Bowling and Condensation, third ed., Clarendon Press, 1994.
[15] CISE, A research program in two-phase flow, CISE final report of works under CAN-1 program, January 1963.
[16] C. Lombardi, L. Maran, L. Oriani, M.E. Ricotti, CESNEF-3 Pressure drop correlation for gas–liquid mixtures flowing upflow in vertical ducts, in: XVIII congresso nazionale della trasmissione del calore, Cernobbio, 28–30 giugno 2000.
[17] K. Stephan, Heat Transfer in Condensation and Boiling, Springer-Verlag, 1992.
[18] G.P. Gaspari, C. Lombardi, G. Peterlongo, Pressare drops in steam–water mixtures, Centro Informazioni Studi Esperienze (CISE) Report R 83, January 1964.
[19] W. Koehler, W. Kastner, Two-phase pressure drop in boiler tubes, in: S. Kakas, A.E. Bergles, E.O. Fernandes (Eds.), Two-Phase Flow Heat Exchangers (Thermal-Hydraulic Fundamentals and Design), Kluwer Academic Publisher, 1988.